

Electrochemical activities of platinum-decorated multi-wall carbon nanotube/chitosan composites for the oxidations of alcohols

Roghayeh Khaleghian-Moghadam ·
Meissam Noroozifar · Mozhgan Khorasani-Motlagh ·
Mehri-Saddat Ekrami-Kakhki

Received: 29 July 2012 / Revised: 29 September 2012 / Accepted: 7 October 2012 / Published online: 17 October 2012
© Springer-Verlag Berlin Heidelberg 2012

Abstract Electrooxidation of alcohols including methanol, ethanol, and isopropanol is studied on the modified solid glassy carbon electrodes with various amounts of platinum nanoparticles (PtNPs) immobilized on a composite of functionalized multi-walled carbon nanotubes (MWCNTs) and chitosan in an acidic solution. Here the chitosan is available as a binder to tightly anchor Pt nanoparticles onto the MWCNTs surfaces. MWCNTs/chitosan composite support can significantly improve the activity of the catalyst for alcohol oxidation and reduce the Pt catalyst loading. The calculated electrochemical active surface area is 379.2 m²/g Pt for PtNP–MWCNT/chitosan. Cyclic voltammetry and chronoamperometry techniques are employed for catalytic activity evaluation. The effects of operational parameters including platinum loading, concentration of the corresponding alcohol, concentration of the acid solution, scanning rate, and the final limit of anodic potential on the performance of the electrodes are also investigated.

Keywords Platinum · MWCNTs · Nanoparticles · Electrooxidation · Alcohol · Chitosan

Introduction

Direct methanol fuel cells (DMFCs) have been recently addressed as one of the most promising energy sources by ever increasing energy demand in the future. Easy handling of methanol as an inexpensive and wildly

available liquid fuel along with the system's simplicity, high-energy density, and low pollutant emission are the most important reasons for scientist's attention to DMFCs [1]. However, there are several major barriers for the practical applications and commercialization of DMFCs. These include limited abundance, high cost, and low activity of noble metal catalysts. Poisoning of the catalysts surface by CO-like species produced during the methanol oxidation process as well as “methanol crossover” to the cathode electrode through the conventionally nafion membrane also need to be considered. Decreasing methanol concentration and employing the modified proton exchange membrane have been addressed as possible ways to overcome the methanol crossover drawback. Recently, aliphatic alcohols such as ethanol, ethylene glycol, and propanol have been examined as renewable liquid energy sources with high energy density and low toxicity [2, 3]. Therefore, direct alcohol fuel cells (DAFCs) operating at low temperature (<100 °C) have been considered as a potential alternative to DMFCs [3].

The electrocatalytic activities of platinum (Pt)-based catalysts depend on many factors, the main factor being the catalyst support. Supporting materials with high surface area are assigned to reduce metal loading while keeping the high activity of the catalyst. In recent years, various carbon-based materials such as carbon black [4–6], activated carbon fibers [7], mesoporous carbon [8], carbon paper [9], and carbon nanotubes [10, 11] have been investigated as catalyst supports. The tubular structure of carbon nanotubes (CNTs) makes them unique among various allotropes of carbon in catalyst support applications. Some of the interesting properties of CNTs include nanometer size, mechanical stability, high electronic and thermal conductivity, and large surface to volume ratio [12]. Since pristine CNTs are chemically

R. Khaleghian-Moghadam · M. Noroozifar (✉) ·
M. Khorasani-Motlagh · M.-S. Ekrami-Kakhki
Department of Chemistry, University of Sistan and Baluchestan,
P.O. Box 98155-147, Zahedan, Iran
e-mail: mnoroozifar@chem.usb.ac.ir

inert, activation of their graphitic surface is often crucial in order to anchor and deposit catalytic nanoparticles [12]. Functionalization of CNTs by an oxidation process using $\text{H}_2\text{SO}_4/\text{HNO}_3$, $\text{H}_2\text{SO}_4/\text{H}_2\text{O}_2$, HNO_3 , O_3 , etc. generates defect sites at the end and/or at the sidewalls of nanotubes. This phenomenon further results in the production of carboxylic groups at the defect sites. This is due to the difference in reactivity between perfect structure and defects [12]. Functionalization process of CNTs will often lead to damage of the tubes. To prevent the harsh conditions of the oxidative treatment of CNTs, an important challenge is the development of methods for increasing adhesion through the CNTs' surface functionalization before deposition of metal nanoparticles. Since CNT functional groups such as $-\text{OH}$ and $-\text{COOH}$ are not homogeneous, Pt crystal seeds may be easily adsorbed on the structural defects, grow on them, and agglomerate which result in the poor utilization of Pt crystals [1]. Numerous studies have focused on the improvement of functionalized CNTs. In situ polymerization of monomers in the presence of CNTs [13] and modifying the CNTs with different polymers [1, 14, 15] are the developing methods used for this purpose. Selvaraj et al. [13] have employed the polypyrrole (ppy)-modified multi-walled carbon nanotube composites as Pt and Pt–Ru nanoparticle catalyst support. Their results denote that activity improvement of the catalyst was due to better metal nanoparticle dispersion in the presence of ppy. Similar results have also been reported for Pt–Co/ppy–CNTs [1].

Chitosan (CH) was selected as a support for heterogeneous catalysts because of its biocompatibility, biodegradability, nontoxicity, as well as conformation and flexibility of the polymer [16, 17]. CH, a product of alkaline deacetylation of the natural polymer chitin, contains both glucosamine and acetyl glucosamine units [17]. These amine groups are responsible for the cationic behavior of chitosan in acidic solutions and its affinity for metal ions. Recently, we reported that modified glassy carbon (GC) with Pt nanoparticles (PtNPs) and CH was active for the oxidation of methanol [18]. The results showed that the dispersion of PtNPs into chitosan membrane (CH) significantly improved the activity of the catalyst for methanol oxidation. In this study, we used functionalized multi-walled carbon nanotubes (MWCNTs) other than chitosan in order to improve the electrode performance. The electro-oxidation of methanol (C_1), ethanol (C_2), and isopropanol (C_3) was studied on the modified glassy carbon electrodes with PtNPs dispersed on the composite of functionalized MWCNTs and chitosan. Cyclic voltammetry (CV) and chronoamperometry (CA) techniques were used to evaluate the activity of the catalysts. The effects of operational parameters on the performance of the electrodes were also investigated.

Experimental

Materials

MWCNTs with nanotube diameters, $\text{OD}=20\text{--}30$ nm, wall thickness = $1\text{--}2$ nm, length = $0.5\text{--}2$ μm and purity $>95\%$ were purchased from Aldrich. $\text{H}_2\text{PtCl}_6 \cdot 6\text{H}_2\text{O}$ and NaBH_4 salts were purchased from Merck and used without further purification. Acetic acid was diluted to a 1 % aqueous solution before use. Chitosan, ([2-amino-2-deoxy-(1-4)- β -D-glucopyranose]), with medium molecular weight of 400,000 Da was purchased from Fluka and was used as received. All solutions were prepared using double distilled water.

Instrumentation

Electrochemical measurements were carried out with a SAMA500 Electroanalyzer system made in SAMA Research Center, Iran. All electrochemical experiments were carried out in a conventional three-electrode cell at room temperature. A platinum electrode and a saturated calomel electrode (SCE) were used as the counter and reference electrodes, respectively. All potentials were measured with respect to this reference electrode at a scan rate of 100 mV s^{-1} . The electrolyte was a mixture of sulfuric acid and the corresponding alcohol with a known concentration. All experiments were performed at room temperature. Transmission electron microscopy (TEM) images were taken using a Philips CM120 transmission electron microscope with 2.5 Å resolutions.

Preparation of PtNP–MWCNTs/CH composites

MWCNTs were first subjected to the oxidative pretreatment by vigorously stirring in a mixture of concentrated sulfuric acid and nitric acid with the volumetric ratio of 3:1 at room temperature for 24 h. This pretreatment removes impurities and generates sufficient functional groups on the surface of MWCNTs [19]. The treated MWCNTs were filtered by centrifugation (2,000 rpm) and washed with double distilled water until the pH of the filtrate reached 7. A solution of chitosan (1 %) in acetic acid (1 %) was prepared based on the literature [20]. In order to produce platinum nanoparticles, metal salts were chemically reduced to their zero valences using NaBH_4 . To reach complete reduction level, the concentration of NaBH_4 used was several times the concentration of the metal salt. The procedure was as follows: 1.5 mg of functionalized MWCNTs was dispersed into the appropriate amount of 1 % chitosan solution using an ultrasonic bath to obtain a uniform carbon ink. A 25 μL of H_2PtCl_6 aqueous solution (0.5 M) was mixed with a known amount of 1 % chitosan solution using a rotary aperture (100 rpm) for 30 min. The prepared carbon ink was added

to the Pt–chitosan mixture and stirred for another 30 min. Then, 50 μL of freshly prepared aqueous solution of 2.5 M NaBH_4 was added to the mixture. The mixture was kept stirring for 90 min to achieve the entire reduction of Pt nanoparticles. The resulting suspension was kept at room temperature for consecutive investigations. In this manner, the PtNPs concentration in the mixture was 4 mM. The same procedure was performed for preparation of the PtNPs–MWCNTs–chitosan composites of 2 and 8 mM PtNPs concentration.

Preparation of the electrodes

The glassy carbon (GC) working electrodes with a 2.5-mm diameter (0.0314 cm^2) were polished with $0.05\text{ }\mu\text{m}$ alumina slurry to a mirror finish surface. After rinsing with double distilled water, they were sonicated in water and 0.5 M H_2SO_4 solution, respectively. The GC electrodes were then transferred to an electrochemical cell for further cleaning and activation by using cyclic voltammetry in the potential range of -1.5 to $+1.5\text{ V}$ vs. SCE at a scan rate of 100 mV s^{-1} in freshly prepared 0.5 M H_2SO_4 solution until a stable cyclic voltammetric profile (≈ 15 times) was obtained. In each case, $10\text{ }\mu\text{L}$ of the prepared corresponding suspension catalyst containing a known amount of 1 % chitosan solution was spread by a pipette onto the prepared glassy carbon substrate. The prepared electrodes were kept at room temperature overnight. During this time, evaporation of the solvent led to the formation of deposited catalyst layer on each GC electrode surface.

Results and discussion

TEM image of PtNPs–MWCNTs–CH composite

TEM image of the composite is shown in Fig. 1. Pt nanoparticles have average diameter of about 2 to 7 nm based on the TEM measurement [18]. From Fig. 1, it can be seen that the Pt nanoparticles have been attached to the most of MWCNTs.

Electrochemical active surface area of the GC/PtNPs–MWCNTs–CH electrodes

The electrochemical active surface area (EASA) of Pt particles is one of the most promising factors for the determination of catalytic activity of the corresponding catalysts, mainly for the oxidation reactions which are surface reactions [10]. EASA of the catalysts could be estimated from the coulombic charge for the hydrogen adsorption and desorption (Q_H) in the background cyclic voltammograms in an acidic solution. In fact, the amount of Q_H is calculated as

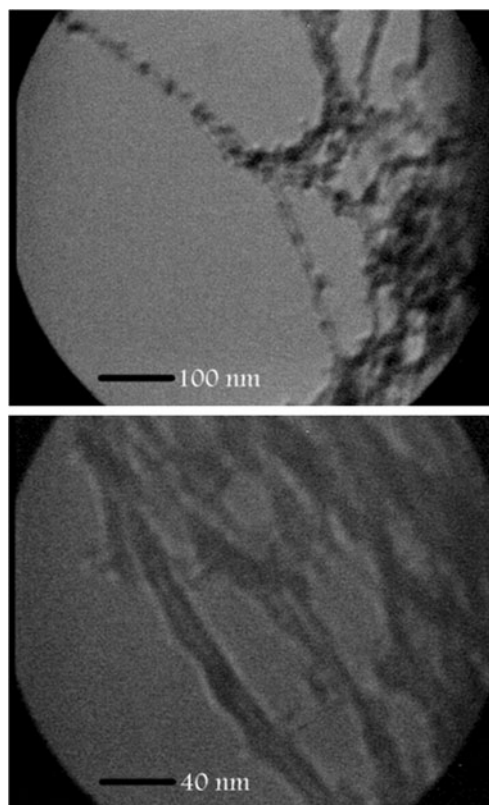


Fig. 1 TEM images of the MWCNTs–PtNPs–CH composites

the mean value of the amounts of charge transfer during the electro-adsorption and desorption of H_2 on Pt sites. The value of EASA is calculated by Eq. 1 [6]:

$$EASA = \frac{Q_H}{0.21 \times [\text{Pt}]} \quad (1)$$

where $[\text{Pt}]$ represents the platinum loading (milligram per square centimeter) in the catalyst, Q_H which represents the charge density for hydrogen desorption (membrane current per square centimeter), and a correlation value of 0.21 which represents the normalized charge density required to oxidize a monolayer of H_2 on polycrystalline Pt catalysts [7, 12, 21].

Figure 2 represents typical cyclic voltammograms for the GC/PtNPs–MWCNTs–CH electrodes containing various amounts of PtNPs (2, 4, and 8 mM) in 0.5 M H_2SO_4 solution at a scan rate of 100 mV s^{-1} and in the potential range of -0.50 to 1.6 V . The features of the CV curves are characteristic of those reported for Pt-based catalysts in an acid solution [22, 23]. For the GC/PtNPs(4 mM)–MWCNTs–CH electrode, fine structures of the hydrogen adsorption/desorption peaks have clearly appeared between -0.07 and -0.34 V , indicating high and ordered dispersion of Pt particles on the catalyst support [6, 7]. A broad peak which appeared in the $+0.70$ to $+1.20\text{ V}$ potential region is attributed to the Pt oxide formation. A reduction peak around $+0.20\text{ V}$, observed during the negative potential scan, is assigned to the reduction of platinum oxide.

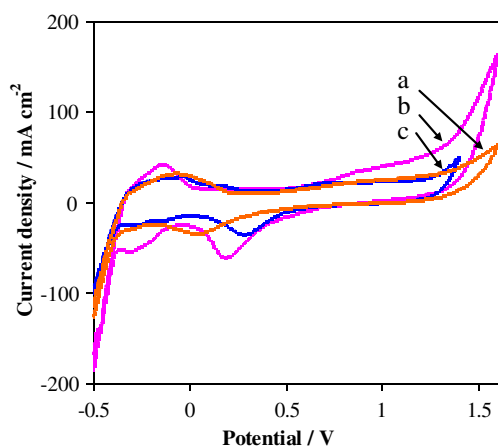


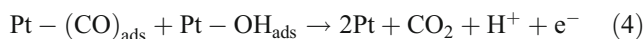
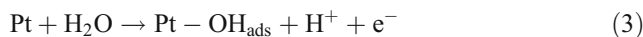
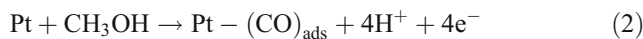
Fig. 2 CV curves of the GC/MWCNTs–PtNPs–CH electrode containing different PtNPs amounts in 0.5 M H₂SO₄: (a) 2, (b) 4, and (c) 8 mM at 100 mV s^{−1}

Based on the background CV shown in Fig. 2b, the amount of EASA of the PtNPs(4 mM)–MWCNTs/CH composite catalyst was calculated ca. 379.17 m²/g Pt. In fact, Q_H was estimated from the area of hydrogen adsorption and desorption region in the background CV (between −0.07 and −0.34 V) and Pt loading in milligram per square centimeter was calculated. Having the amounts of Q_H and [Pt], by Eq. 1, the EASA value of the PtNPs(4 mM)–MWCNTs/CH catalyst was obtained. Similarly, the EASA values of the PtNPs(2 mM)–MWCNTs/CH and PtNPs(8 mM)–MWCNTs/CH catalysts were estimated to be 151.23 and 162.60 m²/g Pt, respectively. Therefore, the EASA of the PtNPs–MWCNTs–CH catalyst containing 4 mM PtNPs is much higher than the other PtNP amounts. This is confirmed from Fig. 2b indicating that the area of hydrogen adsorption and desorption for the PtNPs(4 mM)–MWCNTs/CH is larger than the other two catalysts. The high electrochemical surface area of the catalyst of 4 mM PtNPs loading most likely is attributed to much better dispersion of the Pt particles on the support compared to the catalyst of 8 mM PtNPs loading and superior amount of Pt particles compared to the catalyst of 2 mM PtNPs loading. This result also proposes that Pt particles in the PtNPs(4 mM)–MWCNTs/CH catalyst are in better electronic contact with the MWCNTs surface. In other words, PtNPs loading could affect the electrochemical active surface area of the catalyst. Here, the most appropriate concentration of Pt particles is 4 mM.

Electrooxidation of methanol on the GC/PtNPs–MWCNTs–CH modified electrodes

The electrochemical performance of the GC/PtNPs–MWCNTs–CH electrodes with different amounts of PtNPs toward methanol oxidation was investigated by CV and CA techniques in a 1.0-M methanol and 0.5-M H₂SO₄ solution.

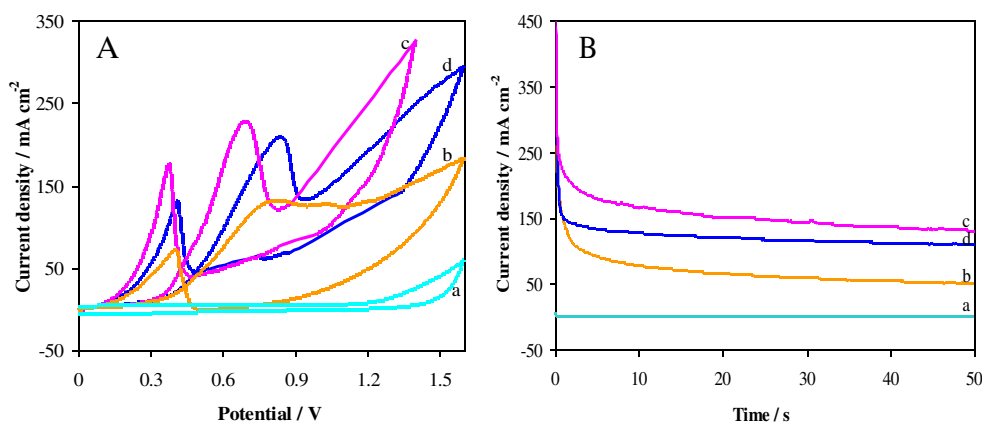
The mechanism for methanol oxidation has been explained by Selvaraj and Alagar [24] (Eqs. 2 to 5).



Methanol is first adsorbed on the metal nanoparticles surface followed by dehydrogenation of the adsorbed species. This results in the formation of strongly adsorbed CO species (Pt–(CO)_{ads}). In order to oxidize such intermediates to CO₂, the adsorbate reacts with the oxygen-containing species in the aqueous solution such as OH_{ads} and H₂O (Eqs. 3 and 4). The slow increase in the current densities at lower potentials during the forward scan could be due to the adsorption of the poisonous intermediates (CO_{ads}), formed in step 1 (Eq. 2), on the platinum surface. The quick increase in the current densities at higher potentials on the forward scan is caused by the partial oxidation of surface platinum to form Pt(OH)_{ads} which helps the conversion of intermediates to carbon dioxide (Eqs. 3 and 4) [24].

The CVs related to methanol oxidation on the GC/PtNPs–MWCNTs–CH electrodes containing different amounts of PtNPs (0, 2, 4, and 8 mM) are shown in Fig. 3a. As seen in Fig. 3a (curve a), no current peaks of methanol oxidation can be observed on the GC/MWCNTs/CH electrode indicating that this electrode has no obvious electrocatalytic activity toward methanol oxidation. This is because no Pt particles have been deposited on the MWCNTs. Similar results were obtained for the GC and GC/CH electrodes whose corresponding CVs have not been represented. As seen in Fig. 3a (curves b–d), two peaks with considerable current density can be observed in the range of 0.0 to 1.6 V for methanol on the GC/PtNPs–MWCNTs–CH electrodes. The peak observed on the forward scan (E_f) at 0.83, 0.70, and 0.86 V, respectively for 2, 4, and 8 mM PtNPs is assigned to the oxidation of methanol. The peak observed on the backward scan (E_b) at 0.38, 0.37, and 0.39 V, respectively for 2, 4, and 8 mM PtNPs concentrations is ascribed to the oxidation of the corresponding intermediates produced during the methanol oxidation process. The characteristics of the CVs and the corresponding potentials are in good agreement with those reported by other researchers [25–27]. The amount of j_f is higher than j_b in all three cases which means that the first step of methanol oxidation reaction is the key step. It is evident from Fig. 3a (curve c) that the peak current density of

Fig. 3 CV curves (a) and CA curves (b) for methanol oxidation on the GC/MWCNTs–PtNPs–CH electrode in 1.0 M methanol and 0.5 M H₂SO₄ with different PtNPs concentrations: (a) 0, (b) 2, (c) 4, and (d) 8 mM



methanol oxidation, i.e., 222.74 mA cm⁻² at the electrode containing 4 mM PtNPs concentration is much higher than those of the other PtNPs concentrations (2 and 8 mM). Moreover, the amount of anodic peak potential, 0.71 V, in the electrode containing 4 mM PtNP concentration is more negative compared to the other Pt amounts. Based on the higher anodic current density and the lower peak potential, the catalyst with 4 mM PtNPs concentration was chosen as the best catalyst among them for the electrooxidation of methanol.

The effect of PtNPs on the anodic peak current density of methanol electrooxidation was also studied by chronoamperometry technique. Typical chronoamperograms for the GC/PtNPs–MWCNTs–CH electrodes containing different amounts of PtNPs, recorded at a potential value of 1.0 V in a 1.0-M methanol and 0.5-M sulfuric acid solution, are shown in Fig. 3b. As it is evident in Fig. 3b (curve a), in the absence of PtNPs, the current–time curve crosses at 0.0 mA cm⁻² amount of current density. This further demonstrates that the GC/MWCNTs/CH electrode has no electrocatalytic activity for methanol oxidation. For the other three cases shown in Fig. 3b (curves b–d), an initial decay of current density can be observed in less than 3 s. However, based on the CA curves, the highest anodic current density was obtained for the GC/PtNPs(4 mM)–MWCNTs/CH electrode. This result is in accordance with that obtained by cyclic voltammetry.

In addition to the amount of PtNPs, other experimental parameters such as methanol and sulfuric acid concentrations, potential scan rate, and potential range can affect the methanol oxidation reaction. Figure 4a shows the effect of methanol concentration on the anodic current density of methanol oxidation on the GC/PtNPs(4 mM)–MWCNTs/CH electrode. It is observed that the anodic peak current density increases with increasing the methanol concentration up to 1.5 M, and there is no significant increase in the peak current density for the methanol concentrations greater than 1.5 M. This could be due to the saturation of the active sites on the surface of the electrode [18, 20].

Also, this indicates that the oxidation of methanol on the modified electrode is controlled by diffusion process [28]. However, the forward peak potential shifts to a more positive direction by increasing the methanol concentration. This phenomenon may be explained by the increase in the poisoning rate of the Pt catalyst by increasing the methanol concentration. This leads to a shift to more positive potentials related to the oxidative removal of the strongly adsorbed intermediates [28].

The effect of sulfuric acid concentration on the anodic peak current density (j_f) and peak potential (E_f) of methanol oxidation was also studied, and the results are represented in Fig. 4b. Regarding the less anodic peak potential and high amount of anodic peak current density, 0.5 M concentration of sulfuric acid was found to be the optimum value in the presence of 1.0 M methanol.

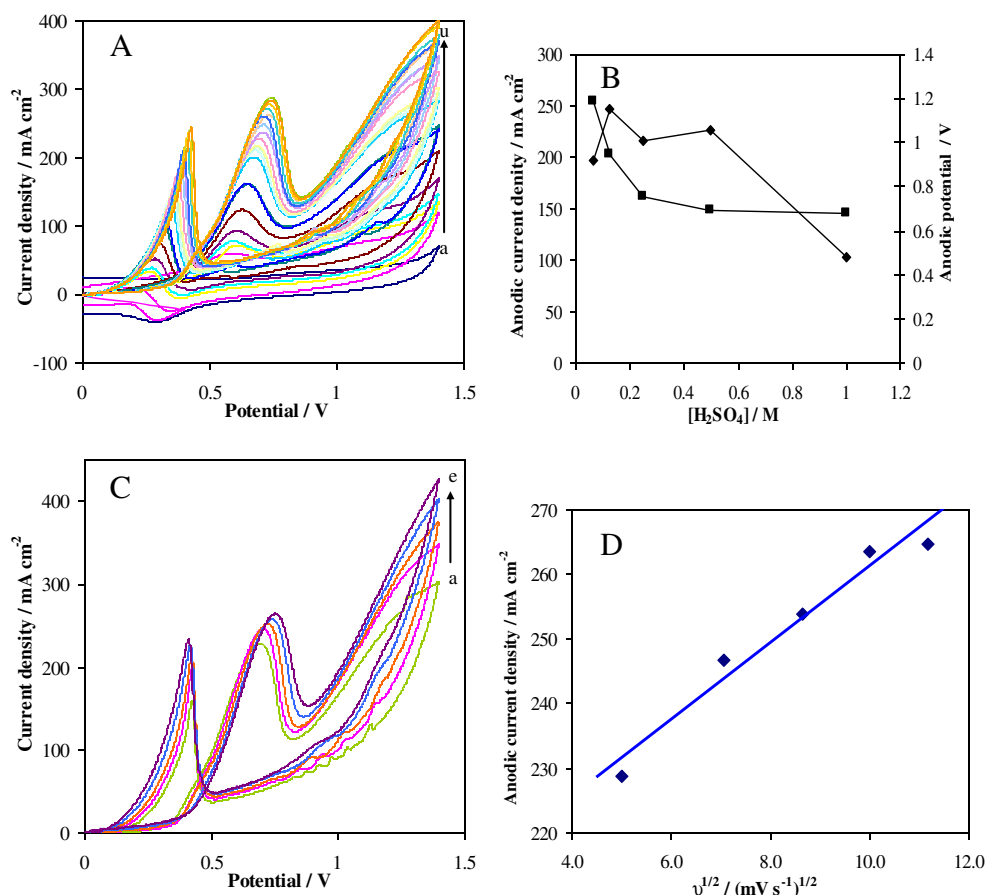
The CV curves were recorded for methanol on the GC/PtNPs(4 mM)–MWCNTs/CH in a mixture of 1.5 M MeOH and 0.5 M H₂SO₄ at various scanning rates of potential in the range of 25–125 mV s⁻¹ (Fig. 4c). Based on these CV curves, the plot of peak current density of methanol oxidation versus the square root of the scan rate was depicted (Fig. 4d). As it is shown in Fig. 4d, by increasing the applied sweeping rate, the anodic peak current density of methanol oxidation slightly moves toward the more positive potential direction. The linear relationship between the square root of the scan rate and the peak current density evaluates further the control of the overall methanol oxidation reaction by the mass transfer of methanol from the bulk solution to the electrode surface.

Electrooxidation of ethanol and isopropanol on the GC/PtNPs–MWCNTs–CH modified electrodes

Electrochemical properties of the GC/PtNPs–MWCNTs–CH electrodes with various amounts of PtNPs (0, 2, 4, and 8 mM) were also investigated for ethanol oxidation by cyclic voltammetry in the presence of a known concentration of the alcohol and 0.125 M H₂SO₄ (Fig. 5a).

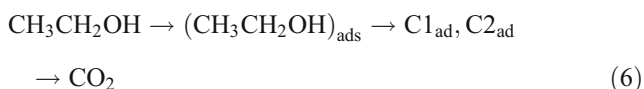
Methanol oxidation reaction (MOR) involves only six electrons and no C–C bond cleavage. This reaction can

Fig. 4 **a** CV curves for methanol oxidation on the GC/MWCNTs–PtNPs–CH in 0.5 M H₂SO₄ at different concentrations of methanol: (a) 0.00, (b) 0.08, (c) 0.16, (d) 0.24, (e) 0.32, (f) 0.39, (g) 0.47, (h) 0.55, (i) 0.62, (j) 0.70, (k) 0.77, (l) 0.85, (m) 0.92, (n) 1.0, (o) 1.07, (p) 1.14, (q) 1.22, (r) 1.30, (s) 1.36, (t) 1.43, (u) 1.50 M. **b** The effect of acid concentration on the anodic current density (diamond) and peak potential (square) of methanol oxidation at the GC/MWCNTs–PtNPs (4 mM)–CH in 1.0 M methanol. **c** CV curves for methanol oxidation on the GC/MWCNTs–PtNPs(4 mM)–CH in 1.5 M MeOH + 0.5 M H₂SO₄ at different scan rates: (a) 25, (b) 50, (c) 75, (d) 100, (e) 125 mV s⁻¹; **d** The plot of the anodic peak current density of methanol oxidation vs. square root of the scan rate (millivolts per second)

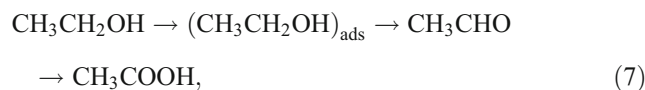


almost completely result in CO₂ production. In contrast to MOR, the mechanism of a complete ethanol oxidation reaction (EOR) on a similar anode catalyst involves 12 electrons and the cleavage of a C–C bond [29]. This bond is between two atoms with little electron affinity which makes the C–C bond cleavage complex at low temperatures [30, 31]. Due to the existence of the C–C bond in ethanol, the entire electrooxidation of ethanol, i.e., ethanol to CO₂, does not easily occur [30]. The EOR undergoes both parallel and consecutive oxidation reactions, resulting in more complicated adsorbed intermediates and byproducts [31]. Ethanol oxidation in acid media occurs through the adsorption of acetyl species and the formation of stable intermediate products such as acetaldehyde and acetic acid [29, 32–35]. On the other hand, the key products are frequently CH₃CHO and CH₃COOH with a little quantity of CO₂ (a few percentage) [30]. Based on the literature [29–34], the overall mechanism of ethanol oxidation in acid media may be summarized in the two parallel reactions (Eqs. 6 and 7):

Total oxidation:



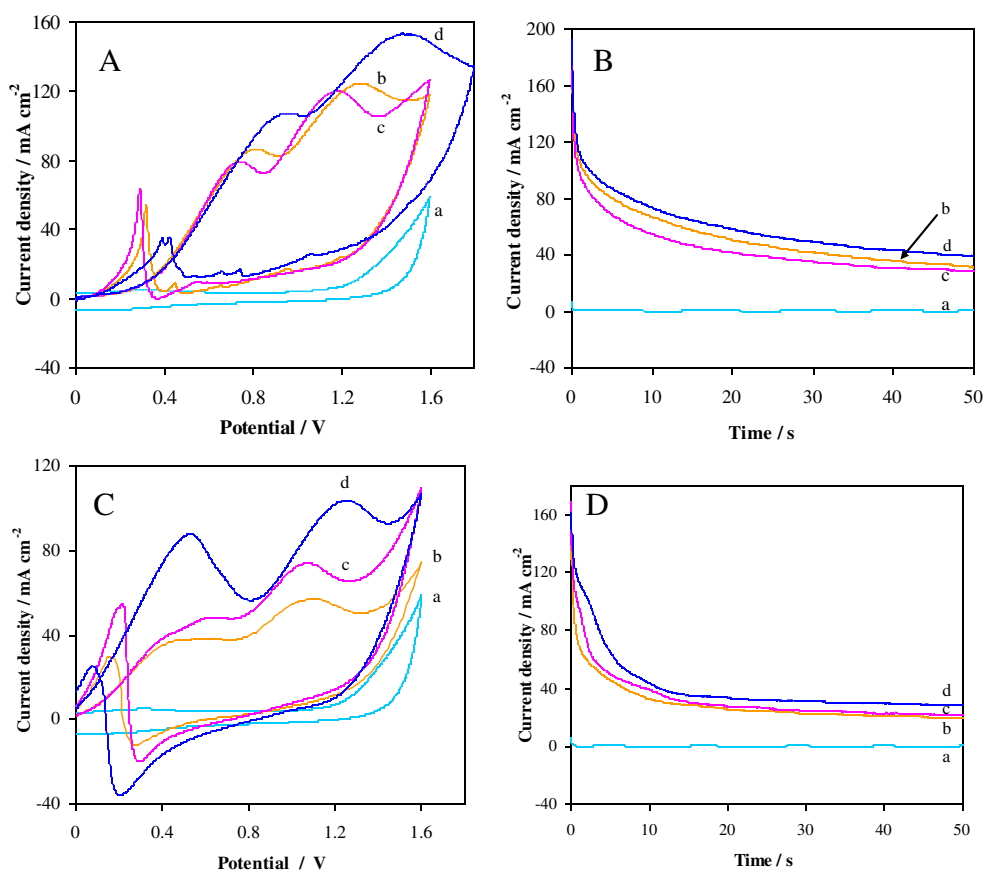
Partial oxidation:



where C1_{ads} and C2_{ads} represent the adsorbed intermediates with one and two carbon atoms, respectively.

As shown in Fig. 5a (curve a), no current peaks of ethanol oxidation can be observed on the GC/MWCNTs/CH electrode with any existence of PtNPs. Similar results were obtained for the GC and GC/CH electrodes whose corresponding CVs have not been shown. The CVs related to ethanol oxidation on the GC/PtNPs–MWCNTs–CH electrodes containing various Pt amounts (2, 4, and 8 mM) in 0.87 M ethanol and 0.125 M sulfuric acid are shown in Fig. 5a (curves b–d), respectively. The features of the CV curves and peak potentials are characteristic of those reported for ethanol oxidation on Pt-based catalysts [35–37]. As seen in Fig. 5a (curves b–d), three peaks with considerable current density are observed in the range of 0.0 to 1.8 V for the three mentioned cases. The two peaks at the forward scan (E_{f1} and E_{f2}), i.e., at 0.83 and 1.3 V for 2 mM PtNPs, 0.74 and 1.19 V for 4 mM PtNPs, as well as 0.96 and 1.50 V for 8 mM PtNPs are assigned to the oxidation of ethanol in two steps (the formation of CO₂ at the first step and the formation of CH₃CHO at the second step [2, 36]).

Fig. 5 CV curves (a) and CA curves (b) for ethanol oxidation on the GC/MWCNTs–PtNPs–CH in 0.87 M EtOH +0.125 M with different PtNPs concentrations: (a) 0, (b) 2, (c) 4, and (d) 8 mM at 100 mV s^{-1} ; CV curves (c) and CA curves (d) for isopropanol oxidation on the GC/MWCNTs–PtNPs–CH in 0.60 M 2-PrOH +0.125 M H_2SO_4 with different PtNPs concentrations: (a) 0, (b) 2, (c) 4, and (d) 8 mM at 100 mV s^{-1}



The peak(s) observed at the backward scan (E_b) at 0.30 V for 2 mM Pt and 0.28 V for 4 mM Pt, as well as two peaks at 0.38 and 0.40 V, respectively for 8 mM PtNPs are ascribed to the removal of the adsorbed intermediates produced during the oxidation process of ethanol [36]. As evident from Fig. 5a (curve d), the peak current densities of ethanol oxidation in two steps at 107.03 and $153.10 \text{ mA cm}^{-2}$ for the electrode containing 8 mM PtNPs loading is higher than the other PtNPs (2 and 4 mM) in 0.125 M H_2SO_4 . However, the amount of anodic peak potentials, 0.96 and 1.50 V, in the case of the electrode of 8 mM PtNPs is more positive compared to the lower PtNPs. Regarding the less anodic peak potentials with considerable anodic peak current densities, i.e., 81.90 and $123.40 \text{ mA cm}^{-2}$, the modified electrode with 4 mM PtNPs loading was referred to the most suitable catalyst for the electrooxidation of ethanol in the present study. Therefore, the rest of the experiments were performed at this Pt loading. The effect of PtNPs on the anodic peak current density of methanol electrooxidation was also studied by chronoamperometry technique. Typical chronoamperograms for the GC/PtNPs–MWCNTs–CH electrodes containing different amounts of PtNPs, recorded at a potential value of 1.0 V in a 0.87-M ethanol and 0.125-M sulfuric acid solution, are shown in Fig. 5b. As it is evident from Fig. 5b (curve a), in the absence of PtNPs, the current–time curve crosses at 0.0 mA cm^{-2} amount of

current density with scanning the time from 0 to 50 s. This further demonstrates that the GC/MWCNTs/CH electrode has no electrocatalytic activity for ethanol oxidation. For the other three cases shown in Fig. 5b (curves b–d), an initial decay of current density can be observed in less than 10 s. Based on the CA curves, the amount of anodic current density for the GC/PtNPs–MWCNTs–CH electrodes containing different amounts of PtNPs was increased in the order of $8 > 2 > 4 \text{ mM PtNPs}$. This result is in accordance with that obtained by cyclic voltammetry.

The electrocatalytic performance of the GC/PtNPs–MWCNTs–CH electrodes with different PtNPs (0, 2, 4, and 8 mM) was also investigated for the oxidation of isopropanol. The electrooxidation mechanism of isopropanol over Pt-based materials in acid solution has been studied using electrochemistry and spectroscopic techniques. Nevertheless, the differences between some of the obtained results by these techniques, the following aspects of the mechanism are in accordance with each other [38]. The only products detected in solution from isopropanol electrooxidation are acetone and carbon dioxide [38]. Isopropanol electrooxidation to form acetone does not involve strongly adsorbed intermediates such as CO, and this reaction begins at lower potentials than the electrooxidation to form CO_2 . The formation of acetone is a surface structure sensitive reaction, and it is significantly faster than the formation of

CO₂ at all potentials [38, 39]. The mechanism of electro-oxidation to form acetone is suggested to occur C–H activation at the alkoxy carbon, and the kinetic of the reaction is fast [39]. Typical CVs obtained in a mixture of 0.60 M isopropanol and 0.125 M H₂SO₄ solution are shown in Fig. 5b. As shown in Fig. 5c (a), no current peaks of isopropanol oxidation can be observed on the GC/MWCNTs/CH electrode. This is because of nonexistence of PtNPs in the catalyst. Similar results were obtained for the GC and GC/CH electrodes whose corresponding CVs have not been shown. The CVs related to isopropanol oxidation on the GC/PtNPs–MWCNTs–CH electrodes containing different loadings of PtNPs (2, 4, and 8 mM) are shown in Fig. 5c (b–d), respectively. As seen in Fig. 5c (b–d), three peaks with considerable current density can be observed in the range of 0.0 to 1.6 V for isopropanol in the three mentioned cases. The two or three peaks at the forward scan are assigned to the oxidation of 2-propanol to acetone and CO₂. The peak(s) observed at the backward scan (E_b) are ascribed to the removal of the adsorbed intermediates produced during the oxidation process of isopropanol [3]. As evident from Fig. 5c (curve d), the peak current densities of isopropanol oxidation in two steps, i.e., 87.43 and 103.50 mA cm⁻² at the GC/PtNPs–MWCNTs–CH electrode containing 8 mM PtNP concentration, are higher than the lower concentrations (2 and 4 mM) in 0.125 M H₂SO₄. However, the amounts of anodic peak potentials, 0.54 and 1.26 V, in the case of the GC/PtNPs(8 mM)–MWCNTs/CH electrodes are more positive compared to the other electrodes. Regardless, the higher anodic current densities of isopropanol oxidation on the GC/PtNP(8 mM)–MWCNTs/CH electrode, for a superior comparison of the results with those of C₁ and C₂ alcohols, the rest of the experiments were performed on the GC/PtNPs(4 mM)–MWCNTs/CH electrode. CA curves for the GC/PtNPs–MWCNT–CH electrodes containing different amounts of PtNPs were also recorded at a potential value of 1.0 V in a 0.60-M isopropanol and 0.125-M sulfuric acid solution which are shown in Fig. 5d. As it is evident in Fig. 5d (curve a), in the absence of PtNPs, the current–time curve crosses at 0.0 mA cm⁻² amount of current density. This exhibits that the GC/MWCNTs/CH electrode has no electrocatalytic activity for isopropanol oxidation. For the other three cases shown in Fig. 5d (curves b–d), an initial decay of current density can be observed in less than 10 s. Based on the CA curves, the amount of anodic current density for the GC/PtNPs–MWCNTs–CH electrodes containing different amounts of PtNPs was increased in the order of 8 > 4 > 2 mM PtNPs. This result is in agreement with that obtained by cyclic voltammetry.

As aforementioned for methanol oxidation experiments, the effects of some parameters such as concentrations of the corresponding alcohol, scan rate, and potential range on the

ethanol and isopropanol oxidation reaction were studied. Figure 6 shows the effect of ethanol and isopropanol concentration on the anodic current density of the corresponding alcohol oxidation on the GC/PtNPs(4 mM)–MWCNTs/CH electrode in a 0.125-M sulfuric acid solution. It is observed that the anodic peak current densities increase with increasing concentration up to 0.87 and 0.58 M for ethanol and isopropanol, respectively. Moreover, no significant increase in the peak current densities is observed at concentrations greater than these concentrations of ethanol and isopropanol. This is because of the saturation of the active sites on the electrode surface. Also, this indicates that the oxidation of ethanol and isopropanol on the electrode surface is controlled by diffusion process [28]. However, the forward peak potentials shifted to a more positive direction as the ethanol and isopropanol concentration increased. As mentioned for the case of methanol, the reason for this is the increase in the poisoning rate of the Pt catalyst by increasing the alcohol concentration [28].

The effect of sweeping rate of potential on the performance of the GC/PtNPs(4 mM)–MWCNTs/CH electrode for ethanol and isopropanol oxidation was investigated using cyclic voltammetry in the mixtures of 0.87 M EtOH + 0.125 M H₂SO₄ (Fig. 7a) and 0.58 M PrOH + 0.125 M H₂SO₄ (Fig. 7c) in the range of 25–150 mV s⁻¹. Based on these CV curves, the plot of peak current densities (j_{pa1} and j_{pa2}) for ethanol oxidation versus the square root of the scan rate were depicted (Fig. 7b, c). It is obvious from Fig. 7b, c that by increasing the scan rate, the anodic peak current densities of ethanol and isopropanol oxidation shift to a more positive direction. The linear relationship between the square root of the scan rate and the forward peak current densities evaluates further that the oxidation reactions of ethanol and isopropanol in both steps are controlled by the diffusion process [10, 28].

The effect of the upper limit of potential in the positive direction on the ethanol and isopropanol electrooxidation at the GC/PtNPs(4 mM)–MWCNTs/CH was also investigated. As it is shown in Fig. 8a, by increasing the final anodic limit of potential from 1.5 to 2.0 V, the amounts of anodic peak current densities slightly increase. On the contrary, the amounts of backward peak potentials (E_b) decrease from 0.33 to 0.21 V by increasing the final potential from 1.5 to 2.0 V. In fact, by increasing the final potential limit, the conversion rate of Pt to PtO is accelerated, which leads to a decrease in j_b . This denotes that ethanol can only be oxidized on the clean surface of a Pt catalyst. Figure 8b represents the effect of the anodic limit of potential on the electrooxidation of isopropanol on the GC/PtNPs(4 mM)–MWCNTs/CH electrode in the potential range of 0.0–1.5 to 0.0–2.0 V in the mixture of 0.58 M isopropanol and 0.125 M H₂SO₄ at the scan rate of 100 mV s⁻¹. As shown in this figure, by increasing the final anodic limit

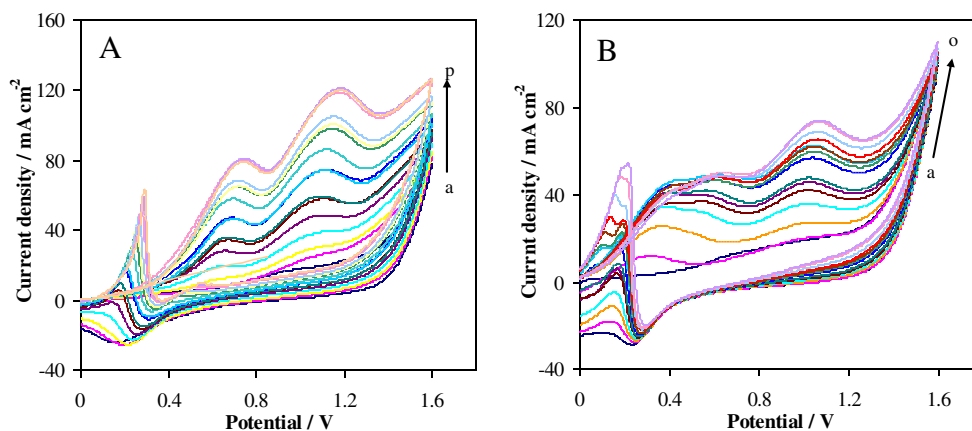


Fig. 6 **a** CV curves for ethanol oxidation on the GC/MWCNTs–PtNPs (4 mM)–CH in 0.125 M H₂SO₄ and different concentrations of EtOH: (a) 0.00, (b) 0.06, (c) 0.11, (d) 0.17, (e) 0.23, (f) 0.28, (g) 0.34, (h) 0.40, (i) 0.45, (j) 0.55, (k) 0.60, (l) 0.66, (m) 0.71, (n) 0.76, (o) 0.82, (p) 0.87 M. **b**

CV curves for isopropanol oxidation on the GC/MWCNTs–PtNPs (4 mM)–CH in 0.125 M H₂SO₄ and different concentrations of isopropanol: (a) 0.00, (b) 0.04, (c) 0.09, (d) 0.13, (e) 0.17, (f) 0.21, (g) 0.25, (h) 0.29, (i) 0.34, (j) 0.38, (k) 0.42, (l) 0.46, (m) 0.50, (n) 0.54, (o) 0.58 M

of potential from 1.5 to 2.0 V, the anodic peak current densities do not change considerably, whereas the backward peak current densities decrease. The backward peak potentials (E_b) also shift toward the less positive direction by increasing the final potential. The reason for this phenomenon is similar to that mentioned for the case of ethanol.

Comparison of the modified electrodes' performance for the electrooxidation of methanol, ethanol, and isopropanol

In the final section of the present study, we investigated the performance of the modified electrodes containing different PtNP amounts (2, 4, and 8 mM) for the C1 to C3 alcohol oxidation in acidic solution using cyclic voltammetry

Fig. 7 **a** CV curves for ethanol oxidation on the GC/MWCNTs–PtNPs–CH in 0.87 M EtOH + 0.125 M H₂SO₄ at different scan rates: (a) 25, (b) 50, (c) 75, (d) 100, (e) 125 and (f) 150 mV s⁻¹. **b** The plots of the anodic peak current densities of ethanol oxidation (j_{pa1} (triangle) and j_{pa2} (diamond)) vs. square root of the scan rate (millivolts per second). **c** CV curves for isopropanol oxidation on the GC/MWCNTs–PtNPs–CH in 0.58 M PrOH + 0.125 M H₂SO₄ at different scan rates: (a) 25, (b) 50, (c) 75, (d) 125, (e) 150 mV s⁻¹. **d** The plot of the anodic peak current density of isopropanol oxidation vs. square root of the scan rate (millivolts per second)

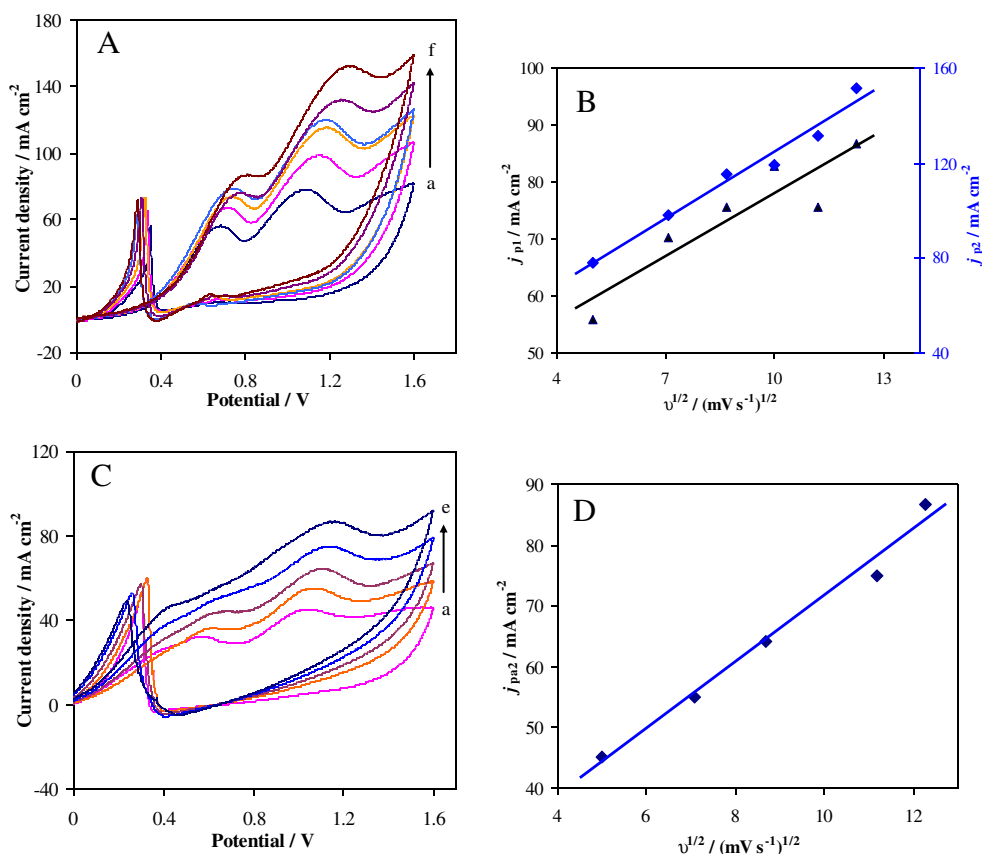
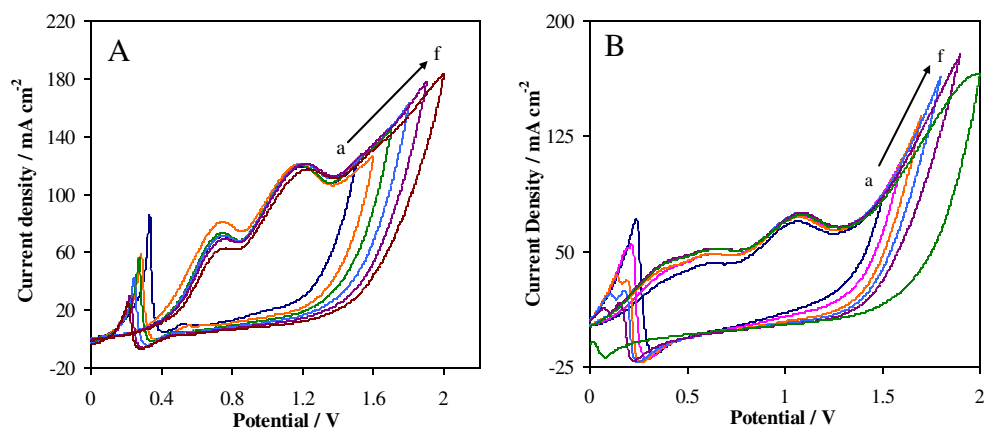


Fig. 8 **a** The effect of upper limit of potential in the positive direction on the ethanol electrooxidation on the GC/PtNPs(4 mM)–MWCNTs–CH in 0.87 M EtOH +0.125 M H₂SO₄ and **b** the isopropanol electrooxidation on the GC/PtNPs(4 mM)–MWCNTs–CH in 0.58 M 2-PrOH +0.125 M H₂SO₄



technique. The data extracted from the related CV curves including the amounts of onset potentials, anodic peak potentials, and anodic peak current densities of methanol, ethanol, and isopropanol in a solution of 0.6 M of the corresponding alcohol and 0.125 M sulfuric acid are summarized in Table 1. The onset potential is the potential at which the alcohol oxidation process begins [40, 41]. In principle, with respect to the alcohol oxidation mechanism, the onset potential is attributed to the cleavage of the C–H bonds and the subsequent removal of the CO_{ads}-like intermediates by oxidation with OH_{ads} supplied by Pt–OH sites [26, 42]. Hence, any shift in the onset potential value to the more negative potential direction reduces the overpotential in the alcohols' oxidation [43]. This caused the alcohol oxidation process to be easier [44] and subsequently the catalytic activity of the corresponding catalyst to increase [6]. As reported in Table 1, the onset potential values are low for electrooxidation of methanol, ethanol, and 2-propanol in three different Pt loading. Moreover, except in the case of the PtNPs(8 mM)–MWCNTs/CH catalyst, the lower the onset potential value, the higher the anodic current density amount which results in the improvement of the catalytic activity. From Table 1, it is evident that regardless of the Pt amounts, the anodic peak current densities for oxidations of all the three alcohols on the GC/PtNPs–MWCNTs–CH electrodes are considerable. However, in

any loading of Pt, the amount of anodic peak current density of methanol oxidation is greater than those of ethanol and 2-propanol. In the case of methanol, the higher anodic peak current density (204.90 mA cm⁻²) and the lower anodic peak potential amounts (0.87 V vs. SCE) and low onset potential (0.15 V) were obtained by the catalyst containing 4 mM PtNP loading. Hence, this Pt loading is the most suitable one for the electrooxidation of methanol in the present study. In the cases of ethanol and 2-propanol, more increases in the anodic peak current densities with a shift to a more positive potential direction were obtained on the GC/PtNPs(8 mM)–MWCNTs/CH electrode compared to the two other electrodes. Overall, except the case of 2-mM PtNP loading, the performance of the GC/PtNPs(4 mM)–MWCNTs/CH and GC/PtNPs(8 mM)–MWCNTs/CH electrodes decreases in the order of methanol > ethanol > 2-propanol. It seems that by increasing the number of carbon atoms in the alcohol structure, the ability of the modified electrodes toward the alcohols oxidation decreases.

In our previous study [18], the incorporation effects of platinum nanoparticles onto the chitosan membrane were discussed in detail. In a solution of 1.0 M methanol and 0.125 M sulfuric acid and at 8-mM PtNP loading, the peak current density and peak potential amounts of methanol oxidation were obtained 166.29 mA cm⁻² and 0.92 V on the GC/PtNPs/CH electrode, respectively [18]. However,

Table 1 The quantitative analysis of cyclic voltammograms for the GC/PtNPs–MWCNTs–CH electrodes containing different amounts of PtNPs in a solution of 0.6 M of corresponding alcohol and 0.125 M H₂SO₄ at a scan rate of 100 mV s⁻¹

Alcohol	PtNP concentration/mM	$E_{\text{onset/V}}$	$E_{\text{pa/V}}$	$j_{\text{pa/mA cm}^{-2}}$	$E_{\text{pa2/V}}$	$j_{\text{pa2/mA cm}^{-2}}$
Methanol	2	0.10	0.97	124.50	–	–
	4	0.15	0.87	204.90	–	–
	8	0.20	1.00	196.00	–	–
Ethanol	2	0.20	0.76	66.94	1.22	98.66
	4	0.21	0.73	64.50	1.16	98.00
	8	0.18	0.85	102.5	1.33	145.3
Isopropanol	2	0.05	0.44	36.80	1.09	56.90
	4	0.01	0.44	40.64	1.07	74.06
	8	0.01	0.55	86.70	1.24	103.50

in the mentioned conditions, the corresponding peak current density and peak potential amounts of methanol oxidation were obtained 247.17 mAcm^{-2} and 0.70 V on the GC/PtNPs–MWCNTs–CH electrode, respectively. In fact, the oxidation peak potential of methanol at the modified GC/PtNPs–MWCNTs–CH electrode shifted by 120 mV to the negative direction compared to the GC/PtNPs/CH electrode. Also, the anodic peak current density at the GC/PtNPs–MWCNTs–CH increased. In comparison, in the presence of functionalized multi-walled carbon nanotubes, the peak current density of methanol oxidation is 1.5 times of current density of methanol oxidation on the GC/PtNPs/CH electrode. The results indicate that the electrocatalytic activity of the GC/PtNPs–MWCNTs–CH is superior than GC/PtNP/CH for methanol oxidation. The increase in the anodic peak current density of methanol oxidation could be attributed to the significant electronic conductivity of the MWCNTs and their greatly electrochemical accessible surface area, as well as a decrease in the amounts of impurities in the carbon support [45]. Also, we compared the activity of the PtNPs(8 mM)–CH (in methanol 1 M, sulfuric acid 0.125 M) with the PtNPs(4 mM)–MWCNTs–CH (in methanol 1 M, sulfuric acid 0.5 M) electrodes for electrooxidation of methanol. For the later case, the corresponding peak current density and peak potential amounts of methanol oxidation were 222.74 mAcm^{-2} and 0.71 V , respectively. In fact, by optimizing the experimental conditions with less Pt loading (4 mM), the anodic peak current density of methanol oxidation was enhanced as 56.45 mAcm^{-2} with a shift to a more negative potential direction as 0.22 V on the PtNP–MWCNTs/CH catalyst compared to the PtNPs–CH catalyst. This result is consistent with the previous reports [46] which characterize the important role of the MWCNTs to disperse the catalyst particles and to reduce the Pt catalyst loading while keeping a high catalytic activity. Moreover, it seems that the composite of MWCNTs/chitosan as the catalyst support can better improve the electrocatalytic properties than the individual counterparts.

Conclusions

A novel MWCNTs-supported PtNPs/chitosan catalyst has been successfully developed for electrooxidation of the C_1 – C_3 alcohols for use in DAFCs. Our results showed that the dispersion of Pt nanoparticles on the functionalized MWCNTs significantly improved the performance of the PtNPs/chitosan composite for the oxidation of the C_1 – C_3 alcohols, especially methanol, and also reduced Pt metal loading in the catalyst. The increase in the catalytic activity toward the alcohol oxidations was attributed to the high surface area and electrical conductivity of the treated MWCNTs which lead to better dispersion of the catalyst

particles and the anodic current density enchantment. Decreasing impurities in the carbon support, the improvement of electrocatalytic properties of the MWCNTs/chitosan composite other than the individual counterparts, as well as a decrease in the poisoning effect of the intermediates produced during the oxidation process also could be considered. This presents a simple and effective approach to produce highly stable Pt catalysts which have a considerable potential for application in DAFCs and other devices.

Acknowledgments We thank University of Sistan and Baluchestan (USB) for the financial support.

References

- Zhao H, Yang J, Li L, Li H, Wang J, Zhang Y (2009) Effect of over-oxidation treatment of Pt–Co/polypyrrole-carbonnanotube catalysts on methanol oxidation. *Int J Hydrogen Energy* 34:3908–3914
- Hosseini J, Bodaghi A (2011) Preparation of palladium nanoparticles–titanium electrodes as a new anode for direct methanol fuel cells. *J Solid State Electrochem* 15:795–800
- Hong KJ, Mook CS, Hoon NS, Ho SM, Hee CS, Bae KW (2008) Influence of Sn content on PtSn/C catalysts for electrooxidation of C_1 – C_3 alcohols: synthesis, characterization, and electrocatalytic activity. *Appl Catal B Environ* 82:89–102
- Jeon MK, Lee KR, Daimon H, Nakahara A, Woo SI (2008) $Pt_{45}Ru_{45}M_{10}/C$ ($M=Fe, Co, \text{ and } Ni$) catalysts for methanol electro-oxidation. *Catal Today* 132:123–126
- Oliveira Neto A, Franco EG, Arico E, Linardi M, Gonzalez ER (2003) Electro-oxidation of methanol and ethanol on Pt–Ru/C and Pt–Ru–Mo/C electrocatalysts prepared by Bönemann's method. *J Eur Ceram Soc* 23:2987–2992
- Liu J, Cao J, Huang Q, Li X, Zou Z, Yang H (2008) Methanol oxidation on carbon-supported Pt–Ru–Ni ternary nanoparticle electrocatalysts. *J Power Sources* 175:159–165
- Huang HX, Chen SX, Yuan C (2008) Platinum nanoparticles supported on activated carbon fiber as catalyst for methanol oxidation. *J Power Sources* 175:166–174
- Joo SH, Pak C, You DJ, Lee S-A, Lee HI, Kim JM, Chang H, Seung D (2006) Ordered mesoporous carbons (OMC) as supports of electrocatalysts for direct methanol fuel cells (DMFC): effect of carbon precursors of OMC on DMFC performances. *Electrochim Acta* 52:1618–1626
- Ahn SH, Kwon OJ, Kim S-K, Choi I, Kim JJ (2010) Electrochemical preparation of Pt-based ternary alloy catalyst for direct methanol fuel cell anode. *Int J Hydrog Energy* 35:13309–13316
- Tong H, Li H-L, Zhang X-G (2007) Ultrasonic synthesis of highly dispersed Pt nanoparticles supported on MWCNTs and their electrocatalytic activity towards methanol oxidation. *Carbon* 45:2424–2432
- Singh RN, Singh A (2009) Anindita Electrochemical activity of binary and ternary composite films of Pd, MWCNT and Ni, Part II: methanol electrooxidation in 1 M KOH. *Int J Hydrog Energy* 34:2052–2057
- Zhao Y, Yang X, Tian J (2009) Electrocatalytic oxidation of methanol at 2-aminophenoxazin-3-one-functionalized multiwalled carbon nanotubes supported PtRu nanoparticles. *Electrochim Acta* 54:7114–7120

13. Selvaraj V, Alagar M (2007) Pt and Pt–Ru nanoparticles decorated polypyrrole/multiwalled carbon nanotubes and their catalytic activity towards methanol oxidation. *Electrochem Commun* 9:1145–1153
14. He D, Mu S, Pan M (2011) Perfluorosulfonic acid-functionalized Pt/carbon nanotube catalysts with enhanced stability and performance for use in proton exchange membrane fuel cells. *Carbon* 49:82–88
15. Kima H-J, Kim W-I, Park T-J, Park H-S, Suh DJ (2008) Highly dispersed platinum–carbon aerogel catalyst for polymer electrolyte membrane fuel cells. *Carbon* 46:1393–1400
16. Du Y, Luo X-L, Xu J-J, Chen H-Y (2007) A simple method to fabricate a chitosan-gold nanoparticles film and its application in glucose biosensor. *Bioelectrochemistry* 70:342–347
17. Guibal E (2005) Heterogeneous catalysis on chitosan-based materials: a review. *Prog Polym Sci* 30:71–109
18. Ekrami-Kakhki M-S, Khorasani-Motlagh M, Noroozifar M (2011) Platinum nanoparticles self-assembled onto chitosan membrane as anode for direct methanol fuel cell. *J Appl Electrochem* 41:527–534
19. Selvaraj V, Vinoba M, Alagar M (2008) Electrocatalytic oxidation of ethylene glycol on Pt and Pt–Ru nanoparticles modified multi-walled carbon nanotubes. *J Colloid Interface Sci* 322:537–544
20. Khorasani-Motlagh M, Noroozifar M, Ekrami-Kakhki M-S (2011) Investigation of nanometals (Ni and Sn) in platinum binary and ternary electrocatalysts for methanol electrooxidation. *Int J Hydrog Energy* 36:11554–11563
21. Maillard F, Martin M, Gloaguen F, Léger JM (2002) Oxygen electroreduction on carbon-supported platinum catalysts. Particle-size effect on the tolerance to methanol competition. *Electrochim Acta* 47:3431–3440
22. Wang S, Jiang SP, White TJ, Wang X (2010) Synthesis of Pt and Pd nanosheaths on multi-walled carbon nanotubes as potential electrocatalysts of low temperature fuel cells. *Electrochim Acta* 55:7652–7658
23. Jang IY, Lee SH, Park KC, Wongwiriyan W, Kim C, Teshima K, Oishi S, Kim YJ, Endo M (2009) Effect of photochemically oxidized carbon nanotubes on the deposition of platinum nanoparticles for fuel cell catalysts. *Electrochem Commun* 11:1472–1475
24. Selvaraj V, Alagar M (2007) Pt and Pt–Ru nanoparticles decorated polypyrrole/multiwalled carbon nanotubes and their catalytic activity towards methanol oxidation. *Electrochem Commun* 9:1145–1153
25. Xu J, Hua K, Sun G, Wang C, Lv X, Wang Y (2006) Electro-oxidation of methanol on carbon nanotubes supported Pt–Fe alloy electrode. *Electrochem Commun* 8:982–986
26. Wu G, Xu B-Q (2007) Carbon nanotube supported Pt electrodes for methanol oxidation: A comparison between multi- and single-walled carbon nanotubes. *J Power Sources* 174:148–158
27. Zhou ZH, Li WS, Fu Z, Xiang XD (2010) Carbon nanotube-supported Pt–H₂MoO₃ as electrocatalyst for methanol oxidation. *Int J Hydrog Energy* 35:936–941
28. He Z, Chen J, Liu D, Zhou H, Kuang Y (2004) Electrodeposition of Pt–Ru nanoparticles on carbon nanotubes and their electrocatalytic properties for methanol electrooxidation. *Diam Relat Mater* 13:1764–1770
29. Fatih K, Neburchilov V, Alzate V, Neagu R, Wang H (2010) Synthesis and characterization of quaternary PtRuIrSn/C electrocatalysts for direct ethanol fuel cells. *J Power Sources* 195:7168–7175
30. Nakagawa N, Kaneda Y, Wagatsuma M, Tsujiguchi T (2011) Product distribution and the reaction kinetics at the anode of direct ethanol fuel with Pt/C, PtRu/C and PtRuRh/C cell. *J Power Sources*. doi:10.1016/j.jpowersour.2-11.10.057
31. Shen SY, Zhao TS, Xu JB (2010) Carbon supported PtRh catalysts for ethanol oxidation in alkaline direct ethanol fuel cell. *Int J Hydrog Energy* 35:12911–12917
32. Colmati F, Antolini E, Gonzalez ER (2006) Effect of temperature on the mechanism of ethanol oxidation on carbon supported Pt, PtRu and Pt₃Sn electrocatalysts. *J Power Sources* 157:98–103
33. Antolini E (2007) Review: catalysts for direct ethanol fuel cells. *J Power Sources* 170:1–12
34. Tayal J, Rawat B, Basu S (2011) Bi-metallic and tri-metallic PtSn/C, PtIr/C, PtIrSn/C catalysts for electro-oxidation of ethanol in direct ethanol fuel cell. *Int J Hydrogen Energy* 36:14884–14897
35. Song H, Qiu X, Li F (2009) Promotion of carbon nanotube-supported Pt catalyst for methanol and ethanol electro-oxidation by ZrO₂ in acidic media. *Appl Catal A Gen* 364:1–7
36. Xiao F, Zhao F, Zeng J, Zeng B (2009) Novel alcohol sensor based on PtRuNi ternary alloy nanoparticles-multi-walled carbon nanotube-ionic liquid composite coated electrode. *Electrochem Commun* 11:1550–1553
37. Thomas JE, Bonesi AR, Moreno MS, Visintin A, Castro Luna AM, Triaca WE (2010) Carbon nanotubes as catalyst supports for ethanol oxidation. *Int J Hydrogen Energy* 35:11681–11686
38. Markiewicz MEP, Hebert DM, Bergens SH (2006) Electro-oxidation of isopropanol on platinum in alkaline electrolytes. *J Power Sources* 161:761–767
39. Cao D, Bergens SH (2003) A direct isopropanol polymer electrolyte fuel cell. *J Power Sources* 124:12–17
40. Kim M, Fang B, Chaudhari NK, Song M, Bae T-S, Yu J-S (2010) A highly efficient synthesis approach of supported Pt–Ru catalyst for direct methanol fuel cell. *Electrochim Acta* 55:4543–4550
41. Cui S-K, Guo D-J (2009) Highly dispersed Pt nanoparticles immobilized on 1,4-benzenediamine-modified multi-walled carbon nanotube for methanol oxidation. *J Colloid Interface Sci* 333:300–303
42. Zhao Y, Yang X, Tian J, Wang F, Zhan L (2010) A facile and novel approach toward synthetic polypyrrole oligomers functionalization of multi-walled carbon nanotubes as PtRu catalyst support for methanol electro-oxidation. *J Power Sources* 195:4634–4640
43. Zhao Y, Yang X, Tian J, Wang F, Zhan L (2010) Methanol electro-oxidation on Ni@Pd core-shell nanoparticles supported on multi-walled carbon nanotubes in alkaline media. *Int J Hydrogen Energy* 35:3249–3257
44. Zhao H, Li L, Yang J, Zhang Y (2008) Co@Pt–Ru core-shell nanoparticles supported on multiwalled carbon nanotube for methanol oxidation. *Electrochem Commun* 10:527–1529
45. Zhang X, Shi X, Wang C (2009) Electrodeposition of Pt nanoparticles on carbon nanotubes-modified polyimide materials for electrocatalytic applications. *Catal Commun* 10:610–613
46. Yang C, Wang D, Hu X, Dai C, Zhang L (2008) Preparation and characterization of multi-walled carbon nanotube (MWCNTs)-supported Pt–Ru catalyst for methanol electrooxidation. *J Alloy Compd* 448:109–115